Measurement of the complex dielectric constant of a single gold nanoparticle

Patrick Stoller,* Volker Jacobsen, and Vahid Sandoghdar

Laboratory of Physical Chemistry, ETH Zurich, 8093 Zurich, Switzerland

Received May 9, 2006; revised May 22, 2006; accepted May 22, 2006;
posted May 25, 2006 (Doc. ID 70731); published July 25, 2006

A differential interference contrast microscopy technique that employs a photonic crystal fiber as a white-light source is used to measure both the real and the imaginary part of the complex dielectric constant of single 10 and 15 nm gold nanoparticles over a wavelength range of 480 to 610 nm. Noticeable deviations from bulk gold measurements are observed at short wavelengths and for individual particles even after taking into account finite-size surface damping effects. © 2006 Optical Society of America

OCIS codes: 290.5850, 300.6550, 180.3170, 260.3910.

Gold nanoparticles exhibit a plasmon resonance peak in the optical absorption and scattering spectrum that is absent from the reflectivity spectrum of bulk gold.[1] Bohren and Huffman[2] presented comparisons between absorption and scattering cross sections calculated from the measured bulk dielectric constant by use of Mie theory[3] and the results of direct measurements on ensembles of nanoparticles smaller than 20 nm. While they found good agreement in general, they observed that the measured absorption peak is broader and lower than that predicted by Mie theory. This discrepancy can be partly explained by a particle-size dependence of the dielectric constant,[1] the main correction being due to an additional damping that arises when the conduction electron mean free path of about 10 nm becomes comparable with the particle size. However, previous studies have noted that a systematic discrepancy between directly measured and calculated absorption values persists even after taking this correction into account.[4–6] Since these measurements have been done on ensembles of gold particles, it is not possible to completely exclude the finite particle size distribution as an explanation of the observed discrepancies. As a result, a few groups have developed methods for the spectroscopy of single gold nanoparticles with diameters below 20 nm.[7–9] None of these, however, has been able to measure independently the real and imaginary parts of the dielectric constant of a single nanoparticle. In this work we combine the detection principle presented in Ref. 7 with a modified version of differential interference contrast (DIC) microscopy[10–12] to achieve this.

The interferometric detection scheme used is sketched in Fig. 1. Quasi-white supercontinuum light generated in a photonic crystal fiber[7] was collimated and then linearly polarized by using a Glan laser polarizer. A phase compensator, consisting of a wavelength-independent Fresnel rhomb polarization rotator followed by an achromatic quarter-wave plate (QWP), allowed adjustment of the phase between light polarized at 45° and 135° angles with respect to the fast axis of the QWP. A Nomarski polarizer, with its fast and slow axes oriented at 45° to those of the QWP was used to generate two beams labeled 1 and 2, separated by an angle of 0.014°. A plan-apochromatic oil-immersion objective (Zeiss 1.4 NA, 63×, DIC) focused the beams into two nonoverlapping spots with orthogonal polarizations on the upper surface of a standard glass coverslip. The light returning from spots 1 and 2 was recombined by the Nomarski polarizer, passed through a confocal pinhole, and subsequently split by a Wollaston polarizer (splitting angle 0.5°) into two linearly polarized components with polarization angles oriented at 0° and 90° with respect to the fast axis of the QWP. As indicated in Fig. 1, if spot 1 contains a particle, the optical field E_1 from this surface is projected onto the positive B (90°) axis and onto the negative A (0°) axis. The field E_2 from the spot without the particle is projected onto the positive A and B axes. Thus, the detectors A and B record the signals $|E_1-E_2|^2$ and $|E_1+E_2|^2$, respectively. The field E_1 consists of the field reflected at the interface and the field $E_p \propto \alpha E_{\mathrm{inc}}$ scattered by the particle, where α is the polarizability of the particle.

Let us now define a complex quantity $X(\omega)$ as

$$X(\omega) \equiv \frac{2}{\pi \epsilon_m d^3}\alpha(\omega) = \frac{\epsilon_p(\omega)-\epsilon_m}{\epsilon_p(\omega)+2\epsilon_m}, \qquad (1)$$

where ω is the frequency of light and ϵ_p, ϵ_m are the dielectric constants of the gold nanoparticle and the

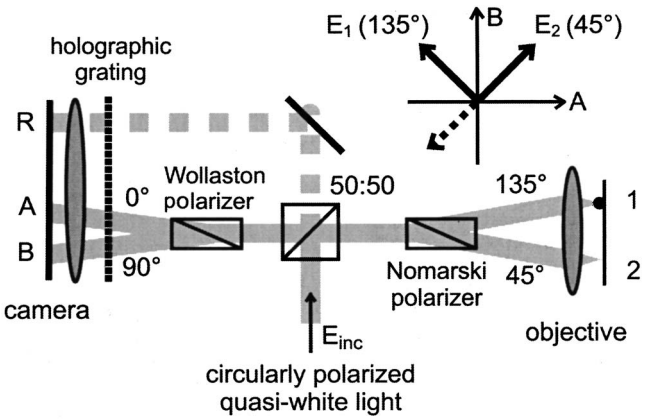

Fig. 1. Illustration of the phase-sensitive detection principle. The polarization angles are specified next to each beam. See text for details.

0146-9592/06/162474-3/$15.00

surrounding medium ($\epsilon_m = 2.30$), respectively. X represents the part of the complex polarizability of a spherical particle that is not directly dependent on the particle size. Following Ref. 12, it can be shown that the real and imaginary components of X are given by the following relations:

$$X_{\mathrm{re}} = \frac{\lambda}{2Cd^3}(A - B), \tag{2}$$

$$X_{\mathrm{im}} = \frac{\lambda}{Cd^3}\left[1 - \sqrt{A + B - 1 - \frac{1}{4}(A - B)^2}\right], \tag{3}$$

where d is the particle diameter, and λ is the wavelength. C is a real proportionality constant that is independent of particle size and wavelength but includes an apparatus function. We calibrated C by measuring the signal from 50 nm silica beads (Polysciences) with a real index of refraction of $n = 1.46$.[13] So starting with the detector signals A and B, we can calculate X_{re} and X_{im} and then solve for the dielectric constant of the gold particles:

$$\epsilon_{\mathrm{re}} = \frac{1 - 2X_{\mathrm{im}}^2 + X_{\mathrm{re}} - 2X_{\mathrm{re}}^2}{X_{\mathrm{im}}^2 + (1 - X_{\mathrm{im}})^2}\epsilon_m, \tag{4}$$

$$\epsilon_{\mathrm{im}} = \frac{3X_{\mathrm{im}}}{X_{\mathrm{im}}^2 + (1 - X_{\mathrm{re}})^2}\epsilon_m. \tag{5}$$

The gold nanoparticles (British Biocell) were spin coated onto coverslips at a density of less than about 1 particle/μm^2. We conducted careful studies to ensure that our sample preparation resulted in single particles, and not aggregates.[7] A drop of immersion oil was placed on top of the coverslip to match its index of refraction. This provides an optically uniform surrounding medium and eliminates any systematic effects on the plasmon spectrum that are due to the substrate. The two beams from the Wollaston traversed a holographic diffraction grating (Kaiser, HFG 550) and were imaged onto a Peltier-cooled CCD camera by an achromatic lens. A spectral resolution of about $\sim$1 nm was readily achieved. As indicated in Fig. 1, a reference beam labeled R from the beam splitter cube was also sent through the diffraction grating and imaged onto the same camera. When the sample was scanned, a camera image with three spectra, A, B, and R, was acquired at each pixel. Spectra A and B were divided by R at each pixel to correct for intensity and spectral fluctuations in the incident light. Particles passing through either of the two focal spots on the sample led to a change in spectra A and B. We note that spectra A, B, and R showed small deviations even without the presence of a particle due to slight chromatic imperfections of the optical components used. To correct for this, the on-particle spectra were normalized further using a background spectrum obtained at a nearby point on the sample without any particles.

In Figs. 2(a) and 2(b), we plot X_{re} and X_{im} as measured on a single 15 nm particle. The solid curves

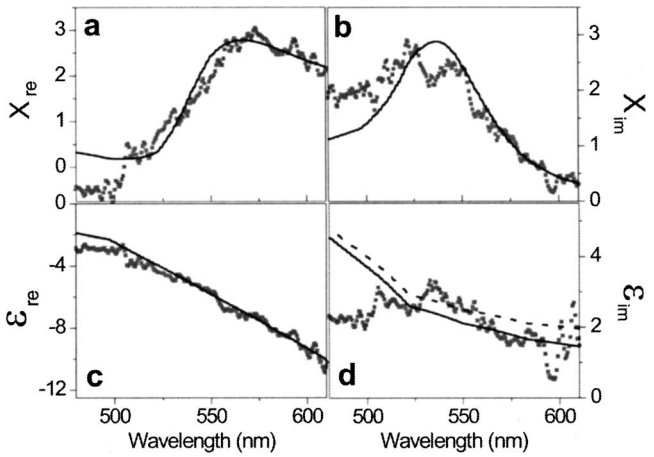

Fig. 2. (a) X_{re} and (b) X_{im} as a function of wavelength for a single 15 nm gold nanoparticle. The solid curve shows the calculated value for a spherical particle in the quasi-static approximation using the bulk dielectric constant of gold. (c) Real and (d) imaginary parts of the dielectric constant calculated from (a) and (b). The solid curve shows the bulk dielectric constant, and the dashed curve shows this quantity corrected for the size-limited mean free conduction electron path.

show the calculated fits from Eqs. (2) and (3) using the bulk dielectric constant of gold taken from the measurements,[14,15] leaving the particle diameter as the only fit parameter. We obtained 10 ± 1 nm for the nominally 10 nm particles and 12 ± 1 nm for the nominally 15 nm particles, while the manufacturer specifies a standard deviation in the particle diameter of $\sim$10% based on transmission electron microscope studies. The symbols in Figs. 2(c) and 2(d) illustrate ϵ_{re} and ϵ_{im} calculated from the data in the upper panels using Eqs. (4) and (5), respectively, whereas the solid curves represent the literature values of bulk gold.[14] We find a clear disagreement between these plots. We note that Muskens *et al.*[9] recently obtained satisfactory fits for the absorption plasmon spectra of small single gold nanoparticles by using $\epsilon_m = 2.04$ and by taking into account the surface damping.[2] Indeed, we would also obtain a better fit for this value of ϵ_m. However, we have chosen to fix the refractive index of the surrounding medium to $\epsilon_m = 2.3$ because we believe this is a well-known parameter of the system.

The particles that we use are likely not perfectly spherical. By using a model that takes into account spheroidal particles, it is possible to obtain somewhat better agreement between measured and calculated values of X_{re} and X_{im} than that shown in Figs. 2(a) and 2(b). The fit results obtained using such calculations give average aspect ratios of 0.74 for both the 10 and 15 nm particles. We analyzed transmission electron microscope images of many 10 nm gold nanoparticles and obtained an estimate of the aspect ratio between 0.8 and 1.0 for all of the particles measured. We thus rule out particle ellipticity as the sole cause for the deviation observed in Figs. 2(a) and 2(b). To compensate for shape-dependent effects on the measured dielectric constant, we averaged over multiple particles of each nominal size (this also re-

duces the fluctuations seen in individual spectra). Figure 3 illustrates the average of ϵ_{re} and ϵ_{im} from thirteen 10 nm particles (blue) and fifteen 15 nm particles (red). For wavelengths longer than about 600 nm, where the plasmon resonance is weak, X_{re} and X_{im} become noisy and cause large fluctuations in ϵ_{re} and ϵ_{im} [see Eqs. (4) and (5)]. In Figs. 3(a) and 3(b) the solid black curves show the real and imaginary values of the bulk dielectric constant, respectively. The blue and red dashed curves in Fig. 3(b) display these quantities after taking into account the limited mean free path of the conduction electrons in 10 and 15 nm particles, respectively. Here we added the surface damping correction term $\frac{3}{4}(\omega_p^2\lambda^3 v_f)/(4\pi^3 c^3 d)$ to ϵ_{im} of bulk gold, where ω_p is the plasma frequency of gold, c is the speed of light in vacuum, and v_f is the electron velocity at the Fermi surface.[2] The data for 10 nm particles are noisier because the signal from these particles is about 3 times smaller than that of 15 nm particles.[7]

Despite the residual intensity and spectral noise in the white-light continuum, it is clear from Fig. 3 that there is good agreement between the real part of the dielectric constant measured in bulk and that measured on 10 and 15 nm particles. Reasonably good correspondence exists between bulk and small particle values of the imaginary part of the dielectric constant in the range of the plasmon resonance, i.e., from about 510 to 580 nm. This agreement is even better when one takes into account the mean free path limitation. However, there is marked disagreement between the bulk and small particle values of ϵ_{im} for wavelengths shorter than about 510 nm. This discrepancy is related to the facts that the measured spectra of X_{im} show a broader and shallower peak than what is calculated and that the measured spectrum of X_{re} dips below the calculated spectrum [see Figs. 2(a) and 2(b)]. The broadening of X_{im}, which corresponds to a broadening in the absorption spectrum, has already been observed in previous studies of ensembles of gold particles.[4] Imperfections of and impurities in the gold nanoparticles and chemical interface damping[16] can both result in additional broadening, but this is difficult to verify for chemically synthesized particles that are coated with surfactants, as used in this work.

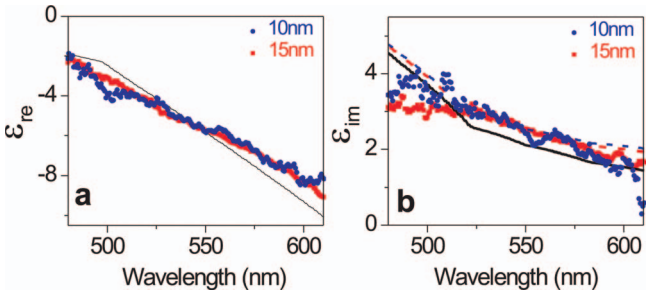

Fig. 3. (a) Real and (b) imaginary parts of the dielectric constant calculated by averaging over fifteen 10 nm particles (blue) and thirteen 15 nm particles (red). The solid curve shows the bulk dielectric constant, and the dashed curves show the same quantity corrected for the size-limited mean free conduction electron path in 10 and 15 nm particles.

To our knowledge, we have reported on the first measurements of both the real and the imaginary parts of the complex dielectric constant of single gold nanoparticles over a broad spectral range. Intensity and spectral noise in the white-light continuum limited the measurement to particles larger than about 10 nm. We are currently working to improve these so we can perform quantitative measurements on single clusters provided by well-controlled fabrication methods.[17] Further measurements would shed light on the deviations of the dielectric constant of small nanoparticles from that of bulk matter.

This work was performed within the Innovations-Initiative (INIT) program of ETH Zurich on Composite Doped Metamaterials. V. Sandoghdar's e-mail address is vahid.sandoghdar@ethz.ch.

*Present address: Institute of Applied Physics, University of Bern, Switzerland.

References

1. U. Kreibig and M. Vollmer, *Optical Properties of Metal Clusters* (Springer, 1995).
2. C. F. Bohren and D. R. Huffman, *Absorption and Scattering of Light by Small Particles* (Wiley, 1983).
3. G. Mie, Ann. Phys. **26**, 329 (1908).
4. R. H. Doremus, J. Chem. Phys. **40**, 2389 (1964).
5. C. G. Granqvist and O. Hunderi, Phys. Rev. B **16**, 3513 (1977).
6. Z. Gu, R. Mu, A. Ueda, M. H. Wu, S. Morgan, W. E. Collins, C. I. Muntele, D. Ila, and B. Vlahovic, Surf. Coat. Technol. **196**, 89 (2005).
7. K. Lindfors, T. Kalkbrenner, P. Stoller, and V. Sandoghdar, Phys. Rev. Lett. **93**, 037401 (2004).
8. S. Berciaud, L. Cognet, P. Tamart, and B. Lounis, Nano Lett. **5**, 515 (2005).
9. O. Muskens, N. Del Fatti, F. Vallee, J. R. Huntzinger, P. Billaud, and M. Boyer, Appl. Phys. Lett. **88**, 063109 (2006).
10. J. S. Batchelder and M. A. Taubenblatt, Appl. Phys. Lett. **55**, 215 (1989).
11. M. A. Taubenblatt and J. S. Batchelder, Appl. Opt. **30**, 4972 (1991).
12. Y. Matsuo and K. Sasaki, J. Acoust. Soc. Jpn. **40**, 6143 (2001).
13. E. Hecht and A. Zajac, *Optics* (Addison-Wesley, 1979).
14. P. B. Johnson and R. W. Christy, Phys. Rev. B **6**, 4370 (1972).
15. R. A. Innes and J. R. Sambles, J. Phys. F: Met. Phys. **17**, 277 (1987).
16. C. Hendrich, J. Bosbach, F. Stietz, F. Hubenthal, T. Vartanyan, and F. Träger, Appl. Phys. B **76**, 869 (2003).
17. U. Kreibig, H. Bönnemann, and J. Hormes, in *Handbook of Surfaces and Interfaces of Materials*, H. S. Nalwa, ed. (Academic, 2001).